

Exploring Adversarial Robustness of LiDAR-Camera Fusion Model in Autonomous Driving

Bo Yang

*College of Electrical Engineering
Zhejiang University
Hangzhou, Zhejiang
yb5@zju.edu.cn*

Xiaoyu Ji

*College of Electrical Engineering
Zhejiang University
Hangzhou, Zhejiang
xji@zju.edu.cn*

Zizhi Jin

*College of Electrical Engineering
Zhejiang University
Hangzhou, Zhejiang
zizhi@zju.edu.cn*

Yushi Cheng

*College of Electrical Engineering
Zhejiang University
Hangzhou, Zhejiang
yushicheng@zju.edu.cn*

Wenyan Xu

*College of Electrical Engineering
Zhejiang University
Hangzhou, Zhejiang
wyxu@zju.edu.cn*

Abstract—Our study assesses the adversarial robustness of LiDAR-camera fusion models in 3D object detection. We introduce an attack technique that, by simply adding a limited number of physically constrained adversarial points above a car, can make the car undetectable by the fusion model. Experimental results reveal that even without changes to the image data channel—and solely by manipulating the LiDAR data channel—the fusion model can be deceived. This finding raises safety concerns in the field of autonomous driving. Further, we explore how the quantity of adversarial points, the distance between the front-near car and the LiDAR-equipped car, and various angular factors affect the attack success rate. We believe our research can contribute to the understanding of multi-sensor robustness, offering insights and guidance to enhance the safety of autonomous driving.

Index Terms—autonomous driving, fusion model, adversarial machine learning, cyber security

I. INTRODUCTION

In recent years, automotive companies have been enhancing the level of automation and intelligence in their vehicles, and the market's acceptance of Autonomous Driving (AD) has grown correspondingly. To earn trust in AD, ensuring its safety is paramount. A primary component of AD is visual perception, which forms the basis for dependable decision-making. The AD system employs sensors like cameras and LiDAR to gather data about the surrounding environment. This data is then processed through deep learning models to achieve perceptions such as object detection.

Cameras and LiDAR are the predominant sensors in AD systems. Both have their own strengths and weaknesses: the more affordable cameras can provide high-resolution images with rich texture details, but are limited in view and depth information, whereas the pricier LiDAR can offer 360° point cloud data with rich depth insights, but the data is unordered and sparse.

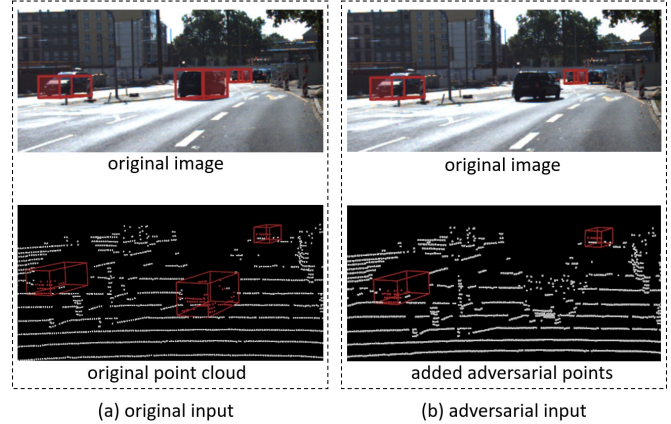


Fig. 1. Adversarial points, when subjected to physical constraints, can deceive the LiDAR-camera fusion 3D detection model used in autonomous driving. By adding a limited number of these adversarial points above the central car, it becomes undetectable by the fusion model.

The AD system typically employs deep neural network-based models to process data collected by sensors, facilitating perception tasks such as object detection. However, deep neural networks have been widely demonstrated to be vulnerable, particularly to adversarial samples [5], [9], [19]. Initially, some studies focused on the safety of camera-only models in AD. Examples include placing patches on stop signs [7] or adding misleading dirt patches on roads [16]. The security challenges related to LiDAR-only models in AD have also garnered attention. Such investigations can be categorized into two approaches: attackers injecting adversarial points into victim LiDAR via a physical-world laser transmitter [4], [12], [18], [22], [22], and the creation or positioning of adversarial 3D objects [21], [24], [25]. However, since both cameras and

LiDAR have their own strengths and weaknesses, a natural idea is to leverage the advantages of both to complement each other. As a result, LiDAR-camera fusion models like Waymo's One and Baidu's Apollo, have emerged. Increasingly, research is addressing the security of these fusion models. In the LiDAR-camera fusion model, data from both sensors serve as the model's input. This presents two data channels—image and points—for potential exploitation by attackers. Some research has focused on introducing disturbances only to image data to impact the fusion model's object detection capabilities [14], others on injecting malicious points solely into LiDAR [10], and still others on strategically positioning objects with adversarial shapes and colors to simultaneously deceive both data channels [2], [3], [20]. However, in a real-world setting, it's challenging to disrupt the image input of the fusion model in an AD system [14]. Moreover, using 3D objects with adversarial features might easily draw the attention of potential victims [3]. It's also tough to guarantee effective deception by introducing random point clouds with an orthographic distribution into the image's field of view [10].

In this work, we aim to explore the security issues associated with the LiDAR-camera fusion model when subjected to adversarial points that satisfy physical constraints. Specifically, for the adversarial points generated at the software level to be injected into the LiDAR via a physical-world laser transmitter, the generation process must adhere to the following three physical constraints: (1) Each laser ray can record at most one point. (2) The vertical angles of adversarial points must align with the laser ray's discrete specific angles. (3) The horizontal angle of adversarial points must be restricted to a narrow range. Using adversarial machine learning methods, we generate points designed to deceive the fusion model. Specifically, we introduce a minimal number of adversarial points above the target vehicle, preventing its detection by the fusion model (referred to as the "Hiding Attack" or HA). Such a strategy may lead to real-world traffic hazards, such as rear-end collisions.

We selected the classic fusion model, MVX-Net [17], to explore its robustness when injected with adversarial points that satisfy physical constraints in the realm of autonomous driving. Experimental results indicate that the LiDAR-camera fusion model remains vulnerable to adversarial points adhering to these physical constraints, even without changes to the image data channel. Furthermore, we delve into how the number, distance, and angle of injected adversarial points affect the performance of the fusion model.

II. BACKGROUND

A. Perception in Autonomous Driving

Perception is the foundational element of autonomous driving, bridging the gap between the vehicle and its environment. Its purpose is to mimic the human eye, collecting relevant information and providing essential data for subsequent decision-making. The overall performance of an autonomous driving system is heavily influenced by the effectiveness of its perception system. Within this framework, object detection

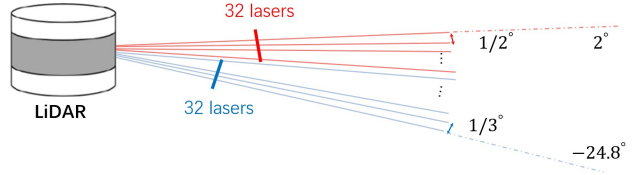


Fig. 2. Velodyne HDL-64E has 64 lasers, and their vertical angle range is -24.8° to 2° . 32 lasers in lower laser block separated by $1/2^\circ$ vertical spacing and 32 lasers in upper laser block separated by $1/3^\circ$ vertical spacing.

(such as detecting pedestrians and cars) serves as a crucial component. To achieve this functionality, autonomous driving vehicles are equipped with multiple sensors across various modalities, along with object detection algorithms that transform sensor data into meaningful semantic information.

B. LiDAR-Camera Fusion 3D Object Detection

In the field of autonomous driving, LiDAR and cameras are the two most common sensors utilized to detect objects in the surrounding environment. However, the data they collect each has its unique strengths and weaknesses. Image data, though rich in texture details, is constrained by its field of view and lacks depth information. On the other hand, the 360-degree point cloud data generated by LiDAR offers valuable depth insights but is disordered and sparse. By fusing data from both LiDAR and cameras, their individual shortcomings can be addressed, leading to a more comprehensive three-dimensional environmental representation. Consequently, object detection based on this fusion is gaining traction, especially in high-level AD vehicles [1]. Existing LiDAR-camera fusion model structures for object detection tasks can be broadly categorized into three types [10]: Cascaded semantic fusion, which utilizes the output of perception from one or multiple sensors to augment the input of other single-sensor perceptions [15], [23]. Integrated semantic fusion, where isolated perception operations are conducted for each sensor and their semantic outputs are then fused [1]. Feature-level fusion, which employs Deep Neural Networks (DNNs) to simultaneously extract and merge image and point features. The resultant combined representation is then processed through a DNN for 3D detection [11], [13], [17].

C. Adversarial Attack in AD

Recently, there has been a surge in interest around adversarial attacks that exploit the vulnerabilities of machine learning algorithms. Researchers have proposed various methods to create adversarial examples (or images) that can lead to misclassifications in 2D image classification and object detection [5], [9], [19]. With the rise of Autonomous Driving (AD), an increasing amount of research is focusing on the safety of perception within the AD system. In particular, adversarial machine learning targeting LiDAR-based 3D object detection is garnering attention [4], [12], [21]. Some studies have delved deeper into such attacks in real-world settings [4], [7], [10], [12], [16], [24], [25]. In the AD domain, prior research has successfully executed real-world adversarial attacks on

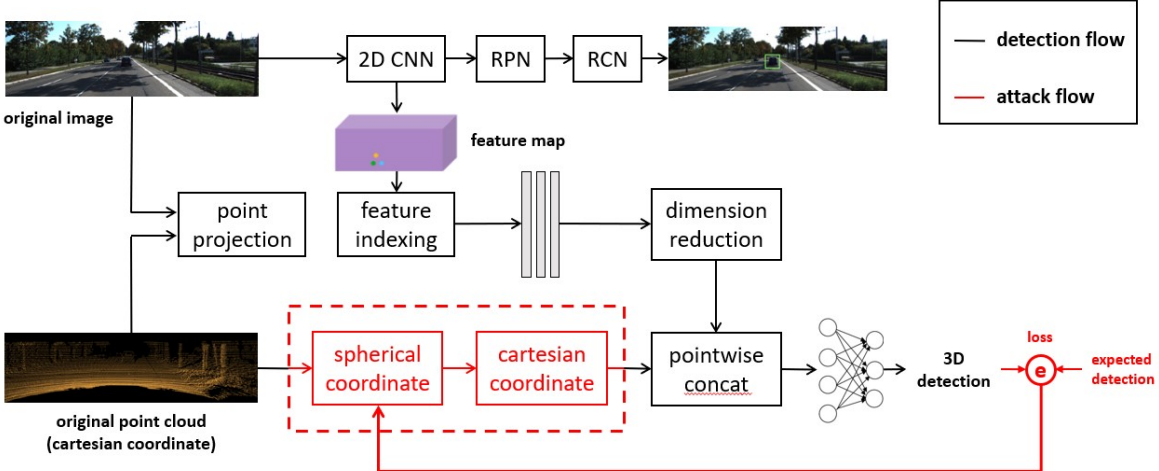


Fig. 3. Overview of the attack pipeline. The standard data processing flow of MVX-Net is indicated by solid black lines. To ensure the injectability of adversarial points into the victim LiDAR in the real world, these points are transformed based on a specific angle in the spherical coordinate system, using the LiDAR as the reference point. This additional data processing step is denoted by a solid red line. The flow of gradients is shown by dashed red lines. As the entire pipeline is differentiable, gradients can flow from the adversarial loss back to the adversarial points within the spherical coordinate system. Ultimately, cars with adversarial points situated above their roofs are rendered undetectable by the fusion model.

camera-based AD perception, such as placing patches on stop signs [7] or deploying deceptive road patches [16]. Other works have targeted LiDAR-based perceptions, either by injecting adversarial points into the target LiDAR via laser transmitters [4], [12] or by designing and positioning adversarial 3D objects [24], [25]. Additionally, some research has explored the impact on target detection accuracy within LiDAR-camera fusion models, particularly by introducing adversarial points into the image cone [10].

III. ATTACK DESIGN

In this work, we aim to place adversarial points atop a car within a 3D scene, ensuring there's no occlusion, with the goal of evading detection by the LiDAR-camera fusion model. We only modify the LiDAR data input channel of the fusion model. The physical constraints for the adversarial points, as determined by the LiDAR acquisition data, are maintained by merely adjusting the adversarial points' coordinates within the spherical coordinate system (see Fig. 3). We employ this attack to analyze how these adversarial points impact the car detection accuracy of an AD's LiDAR-camera 3D detection model. Our focus is on car detection, given its significance as one of the most safety-critical tasks in an AD's perception system. In the following sections, we elaborate on the threat model, physical constraints, victim models, attack objective function, and the optimization process.

A. Threat Model

We assume an attack scenario as follows: The attacker hides in a concealed position on the road and uses laser transmitters to inject adversarial points into passing vehicles. The goal is to deceive the LiDAR-camera fusion model deployed on the victim vehicle, rendering the front-near cars undetectable. Such a deception could lead to severe traffic incidents, including rear-end collisions. Furthermore, the attacker is knowledgeable

about adversarial machine learning and has access to the fusion model's relevant parameters. They can also obtain the model's output results (e.g., Apollo is an open source autopilot framework). Specifically, the adversary has the capability to consistently inject over 200 adversarial points, with the horizontal angle range of the injected adversarial point cloud being less than 10°.

B. Physical Constraint

The point cloud space is sparse. Every generated point can only reside on one of the sparse LiDAR's laser rays, and each laser ray can record at most one point. Therefore, to ensure that the LiDARs can perceive adversarial points emitted by the adversary's transmitter in the real world, we must ensure that the added adversarial points align with these laser rays. Specifically, we adhere to the following physical constraints when generating adversarial points:

- **Each laser ray can record at most one point.** Autonomous vehicles equipped with LiDARs often operate under the Strongest Return Mode setting [4]. In this mode, each laser only records the point with the highest reflection intensity. Without proper constraints on the adversarial points, there might arise a situation where two adversarial points appear on the same laser ray, violating physical reality.
- **The vertical angles of the adversarial points must align with the laser ray's discrete specific angles.** Common mechanical LiDARs used in AD come in configurations like 16-line, 32-line, 64-line, and so on (refer to Fig. 2). These laser beams are distributed at specific vertical angles centered on the LiDAR. As a result, it's crucial to ensure that the added adversarial points fall within these preset angles.
- **The horizontal angle of the adversarial points must be restricted to a narrow range.** The attacker's capabilities

are bound by hardware constraints, such as the laser transmitter. As such, it's infeasible to inject adversarial points across the full 360° horizontal angle of the target LiDAR simultaneously. Currently, attackers can generally introduce adversarial points within a 10° horizontal angle distribution.

C. Victim Models

We selected the MVX-Net model [17] for our experiments to investigate its detection performance in the presence of adversarial points constrained by physical limitations. MVX-Net is a classic feature-level fusion model. It employs convolutional filters from a pre-trained 2D faster RCNN to compute the image feature map. The 3D points are projected onto the image using calibration data, and the corresponding image features are appended to these 3D points.

D. Attack Objective Function

The adversary's goal is to add adversarial points atop the targeted object, making it undetectable. Our strategy involves suppressing bounding box proposals related to the targeted objects. A proposal near the targeted object is considered relevant if it meets two criteria: its Intersection over Union (IoU) is above a specified threshold, denoted as ϵ_i , and the confidence level in class prediction for the proposal exceeds a certain threshold, denoted as ϵ_s . Considering the complexities of real-world attacks, we choose to place adversarial points above the targeted object. This approach aims to suppress relevant proposals while avoiding possible occlusions or interferences caused by the targeted object itself. Therefore, we have devised our attack objective function in this manner:

$$\mathcal{L}_{adv} = \sum_{p,c \in P} \text{IoU}(p^{gt}, p) \log(c) \quad (1)$$

where $P = \{(x_i, y_i, z_i, d_i, w_i, h_i, rot_i, c_i) | i \in [1, n]\}$ represents the set of all bounding box proposals; n is the total number of these adversarial point proposals; p^{gt} denotes the actual position of the targeted object, and p and c are the relevant bounding box proposals and their confidences, respectively. In our approach, $\epsilon_i = 0.1$ and $\epsilon_s = 0.1$.

E. Optimization Process

The process for generating adversarial points, while adhering to physical constraints, is outlined in Algorithm 1. We restrict the space for adding adversarial points to a $3.6 \times 3.6 \text{ m} \times 1\text{m}$ region above the car we aim to obscure. Within this space, we calculate the allowable variations in distance, vertical angle, and horizontal angle for the adversarial points based on spherical coordinates.

During optimization, to ensure the adversarial points comply with physical constraints, we update the distance of these points using the gradient information from the function's backpropagation within the spherical coordinate system. However, we do not adjust the vertical and horizontal angles of the adversarial points based on gradient information. This

Algorithm 1: Generating adversarial points under physical constraints

```

Input: clean point cloud :  $P$ 
      expected location :  $\text{Loc}^{exp}$ 
      number of adversarial points:  $n$ 
      number of initialization times :  $n_{init}$ 
      number of optimization iteration :  $n_{iter}$ 
1 for  $j \in \{1, 2, 3, \dots, n_{init}\}$  do
2   randomly initialize adversarial points
3    $P_{adv} = \{(R'_i, \alpha'_i, \omega'_i) \in \text{Loc}^{exp} | i \in [1, n]\}$ 
4    $P' \leftarrow P + P_{adv}$ 
5   for  $k \in \{1, 2, 3, \dots, n_{iter}\}$  do
6     convert  $P_{adv}$  to spherical coordinate  $P_{adv}$ 
7     convert  $P_{adv}$  to Cartesian coordinates  $P_{adv}$ 
8     get detection result:  $M(P_{adv})$ 
9     if  $\text{Obj}^{exp}$  undetected :
10      break
11      calculate  $\delta'$  by function ???
12      update  $P_{adv} \leftarrow P_{adv} + \delta'$ 
13      convert  $P_{adv}$  to Cartesian coordinates  $P_{adv}$ 
14      update  $P' \leftarrow P + P_{adv}$ 
15   end
16   if  $\text{Obj}^{exp}$  undetected :
17     break
17 end
Output: adversarial point cloud :  $P_{adv}$ 

```

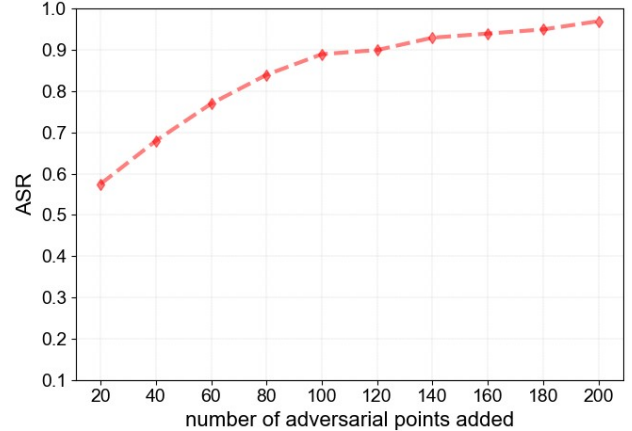


Fig. 4. Attack success rate of spoofing fusion model to make front-near cars undetected with different number of adversarial points. The ASR roughly increases with the number of added adversarial points.

constraint ensures that each laser ray captures at most one point.

The initial vertical and horizontal angles of the adversarial points in the spherical coordinate system are set during random initialization. To mitigate the impact of this randomness, we permit the adversarial points to be re-initialized n_{init} times during the optimization process.

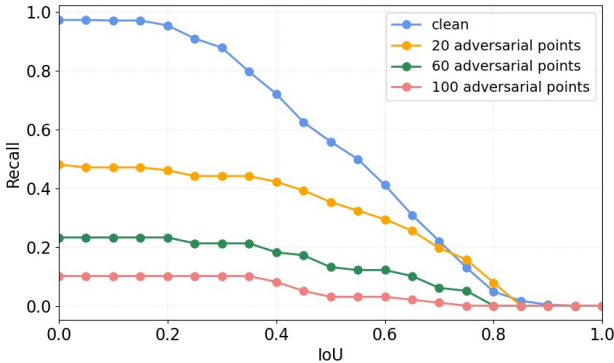


Fig. 5. Recall-IoU curves with different IoU thresholds. The curve labeled with "clean" represents the performance of the fusion model MVX-Net [17] without interference from adversarial points that comply with physical constraints.

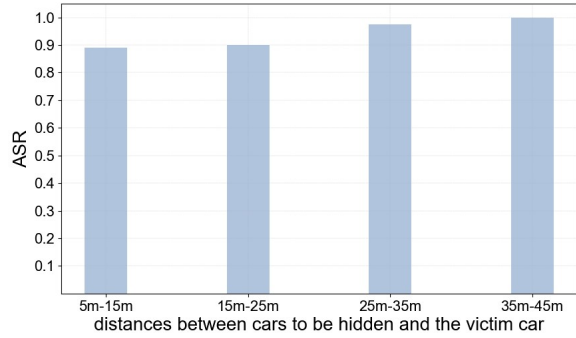


Fig. 6. Attack success rate of spoofing fusion model with different distances between cars to be hidden and the victim car deployed with LiDAR.

IV. EVALUATION

We assess the efficacy of adversarial points under physical constraints in deceiving the LiDAR-camera fusion model. Our focus is on car detection, a safety-critical task in AD's perception system. Specifically, we aim to add adversarial points above the car, constrained physically, to make it undetectable by the fusion model. Our evaluation metric is the attack success rate (ASR), which is the ratio of successful attacks against an object detector to the total number of attacks made. We also examine the relationship between recall and the IoU threshold during the attack. Moreover, we investigate the effects of the number, distance, and angle of injected adversarial points on the fusion model's performance.

A. Experimental Setup

We employ the KITTI [8] dataset for simulation evaluation, a staple in training and testing 3D object detectors. As reiterated, our primary concern is car detection due to its critical safety implications in AD's perception system. The security of the LiDAR-camera fusion model MVX-Net [17] is evaluated using the implementation from MMDetection3D [6].

We set up the aforementioned object detectors in our lab, utilizing a server powered by an Intel Xeon Gold 6240C CPU @2.60 GHz, equipped with four GeForce RTX 3090 GPUs, and furnished with 256 GB of RAM. This setup is utilized for optimizing adversarial point clouds.

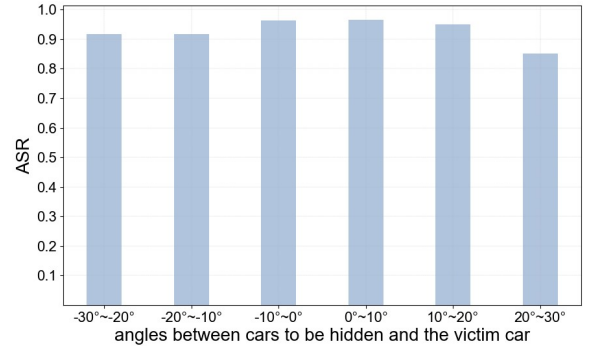


Fig. 7. Attack success rate of spoofing fusion model with different angle between cars to be hidden and the victim car deployed with LiDAR.

B. Number of Added Adversarial Points

To discern the impact of different numbers of adversarial points on the fusion model's detection capabilities, we randomly select 100 cars from the KITTI dataset with the intent to render them undetectable. Fig. 4 depicts the ASR's progression as a function of the number of adversarial points added. With 20 adversarial points, the ASR stands at 39%, but with 200 points, it escalates to 99%. Generally, the ASR shows a positive correlation with the number of added adversarial points. However, its growth rate decelerates once the count surpasses 100. These findings corroborate that physically constrained adversarial points can effectively deceive the LiDAR-camera fusion model. Furthermore, as can be seen from Figure 5, after the addition of adversarial points, the model's recall drops significantly. With the increase in the number of adversarial points, the recall is even lower at the same IoU. This indicates that the robustness of the MVX-Net [17] is notably compromised when interfered with by adversarial points.

C. Influence of Distance

We explored the impact of distance between the cars intended to be concealed and the victim car equipped with LiDAR on the ASR. We randomly selected 1016 cars, which the fusion model detected with high confidence from the KITTI dataset, to serve as concealed targets. Among these, 263 cars are 5m-15m away from the LiDAR, 376 cars are 15m-25m, 234 cars are 25m-35m, and 143 cars are 35m-45m. The results are shown in Fig. 6.

Interestingly, the greater the distance of the adversarial points from the LiDAR, the higher the ASR. This suggests that cars farther away from the victim vehicle with LiDAR are easier to make undetectable by introducing adversarial points above them. This is because a closer car will typically send more reflected rays to the LiDAR, resulting in more recorded points and preserved features. Hence, the fusion model will detect the closer car with higher confidence, making it harder to conceal with adversarial points.

D. Influence of Angle

We also examined the impact of the angle between the cars intended to be hidden and the victim car equipped with LiDAR

on the ASR. From the KITTI dataset, we randomly selected 950 cars detected with high confidence by the fusion model to be concealed. Among these 950 cars, there are 73 cars to be hidden within the angle from -30° to -20° of the victim car, 158 cars within the angle from -20° to -10° , 282 cars within the angle from -10° to 0° , 204 cars within the angle from 0° to 10° , 139 cars within the angle from 10° to 20° , 94 cars within the angle from 20° to 30° . The results are illustrated in Fig. 7. The smaller the angle between the car intended to be concealed and the victim car (the more the car is directly in front of the victim car, with 0° being exactly in front), the higher the ASR. This aligns with adversarial expectations, as an attacker would ideally want the concealed vehicle directly in front of the victim vehicle, increasing the likelihood of abrupt braking and potential rear-end collisions.

V. CONCLUSION

In our research, we investigate the adversarial robustness of the LiDAR-camera fusion model in autonomous driving, particularly when injected with adversarial points that adhere to physical constraints. We discovered that by adding a limited number of adversarial points above a car, the fusion model can be deceived into not detecting the car. Intriguingly, this vulnerability exists even when only the LiDAR data channel is modified, without tampering with the image data channel. This finding highlights a significant safety concern in autonomous driving. Our results indicate that the Attack Success Rate tends to increase with the quantity of introduced adversarial points. Moreover, the greater the distance between the adversarial points and the victim car equipped with LiDAR, the higher the ASR for concealing cars. Additionally, we observed that cars positioned closer to the front of the victim vehicle are more easily rendered undetectable by the fusion model when adversarial points are added. We hope that our findings offer valuable insights into the robustness of multi-sensor systems, contributing to safer autonomous driving solutions.

REFERENCES

- [1] <https://www.apollo.auto/>.
- [2] M. Abdelfattah, K. Yuan, Z. J. Wang, and R. Ward, “Adversarial attacks on camera-lidar models for 3d car detection,” in *2021 IEEE/RSJ International Conference on Intelligent Robots and Systems (IROS)*. IEEE, 2021, pp. 2189–2194.
- [3] Y. Cao, N. Wang, C. Xiao, D. Yang, J. Fang, R. Yang, Q. A. Chen, M. Liu, and B. Li, “Invisible for both camera and lidar: Security of multi-sensor fusion based perception in autonomous driving under physical-world attacks,” in *2021 IEEE Symposium on Security and Privacy (SP)*. IEEE, 2021, pp. 176–194.
- [4] Y. Cao, C. Xiao, B. Cyr, Y. Zhou, W. Park, S. Rampazzi, Q. A. Chen, K. Fu, and Z. M. Mao, “Adversarial sensor attack on lidar-based perception in autonomous driving,” in *Proceedings of the 2019 ACM SIGSAC conference on computer and communications security*, 2019, pp. 2267–2281.
- [5] N. Carlini and D. Wagner, “Towards evaluating the robustness of neural networks,” in *2017 ieee symposium on security and privacy (sp)*. IEEE, 2017, pp. 39–57.
- [6] M. Contributors, “MMDetection3D: OpenMMLab next-generation platform for general 3D object detection,” <https://github.com/open-mmlab/mmdetection3d>, 2020.
- [7] K. Eykholt, I. Evtimov, E. Fernandes, B. Li, A. Rahmati, C. Xiao, A. Prakash, T. Kohno, and D. Song, “Robust physical-world attacks on deep learning visual classification,” in *Proceedings of the IEEE conference on computer vision and pattern recognition*, 2018, pp. 1625–1634.
- [8] A. Geiger, P. Lenz, C. Stiller, and R. Urtasun, “Vision meets robotics: The kitti dataset,” *International Journal of Robotics Research (IJRR)*, 2013.
- [9] I. J. Goodfellow, J. Shlens, and C. Szegedy, “Explaining and harnessing adversarial examples,” *arXiv preprint arXiv:1412.6572*, 2014.
- [10] R. S. Hallyburton, Y. Liu, Y. Cao, Z. M. Mao, and M. Pajic, “Security analysis of {Camera-LiDAR} fusion against {Black-Box} attacks on autonomous vehicles,” in *31st USENIX Security Symposium (USENIX Security 22)*, 2022, pp. 1903–1920.
- [11] T. Huang, Z. Liu, X. Chen, and X. Bai, “Epnnet: Enhancing point features with image semantics for 3d object detection,” in *Computer Vision-ECCV 2020: 16th European Conference, Glasgow, UK, August 23–28, 2020, Proceedings, Part XV 16*. Springer, 2020, pp. 35–52.
- [12] Z. Jin, X. Ji, Y. Cheng, B. Yang, C. Yan, and W. Xu, “Pla-lidar: Physical laser attacks against lidar-based 3d object detection in autonomous vehicle,” in *2023 IEEE Symposium on Security and Privacy (SP)*. IEEE, 2023, pp. 1822–1839.
- [13] J. Ku, M. Mozifian, J. Lee, A. Harakeh, and S. L. Waslander, “Joint 3d proposal generation and object detection from view aggregation,” in *2018 IEEE/RSJ International Conference on Intelligent Robots and Systems (IROS)*. IEEE, 2018, pp. 1–8.
- [14] W. Park, N. Liu, Q. A. Chen, and Z. M. Mao, “Sensor adversarial traits: Analyzing robustness of 3d object detection sensor fusion models,” in *2021 IEEE International Conference on Image Processing (ICIP)*. IEEE, 2021, pp. 484–488.
- [15] C. R. Qi, W. Liu, C. Wu, H. Su, and L. J. Guibas, “Frustum pointnets for 3d object detection from rgb-d data,” in *Proceedings of the IEEE conference on computer vision and pattern recognition*, 2018, pp. 918–927.
- [16] T. Sato, J. Shen, N. Wang, Y. Jia, X. Lin, and Q. A. Chen, “Dirty road can attack: Security of deep learning based automated lane centering under Physical-World attack,” in *30th USENIX Security Symposium (USENIX Security 21)*. USENIX Association, Aug. 2021, pp. 3309–3326. [Online]. Available: <https://www.usenix.org/conference/usenixsecurity21/presentation/sato>
- [17] V. A. Sindagi, Y. Zhou, and O. Tuzel, “Mvx-net: Multimodal voxelnet for 3d object detection,” in *2019 International Conference on Robotics and Automation (ICRA)*. IEEE, 2019, pp. 7276–7282.
- [18] J. Sun, Y. Cao, Q. A. Chen, and Z. M. Mao, “Towards robust lidar-based perception in autonomous driving: General black-box adversarial sensor attack and countermeasures,” in *29th {USENIX} Security Symposium ({USENIX} Security 20)*, 2020, pp. 877–894.
- [19] C. Szegedy, W. Zaremba, I. Sutskever, J. Bruna, D. Erhan, I. Goodfellow, and R. Fergus, “Intriguing properties of neural networks,” *arXiv preprint arXiv:1312.6199*, 2013.
- [20] J. Tu, H. Li, X. Yan, M. Ren, Y. Chen, M. Liang, E. Bitar, E. Yumer, and R. Urtasun, “Exploring adversarial robustness of multi-sensor perception systems in self driving,” *arXiv preprint arXiv:2101.06784*, 2021.
- [21] J. Tu, M. Ren, S. Manivasagam, M. Liang, B. Yang, R. Du, F. Cheng, and R. Urtasun, “Physically realizable adversarial examples for lidar object detection,” in *Proceedings of the IEEE/CVF Conference on Computer Vision and Pattern Recognition*, 2020, pp. 13 716–13 725.
- [22] X. Wang, M. Cai, F. Sohel, N. Sang, and Z. Chang, “Adversarial point cloud perturbations against 3d object detection in autonomous driving systems,” *Neurocomputing*, vol. 466, pp. 27–36, 2021.
- [23] Z. Wang and K. Jia, “Frustum convnet: Sliding frustums to aggregate local point-wise features for amodal 3d object detection,” in *2019 IEEE/RSJ International Conference on Intelligent Robots and Systems (IROS)*. IEEE, 2019, pp. 1742–1749.
- [24] K. Yang, T. Tsai, H. Yu, M. Panoff, T.-Y. Ho, and Y. Jin, “Robust roadside physical adversarial attack against deep learning in lidar perception modules,” in *Proceedings of the 2021 ACM Asia Conference on Computer and Communications Security*, 2021, pp. 349–362.
- [25] Y. Zhu, C. Miao, T. Zheng, F. Hajiaghajani, L. Su, and C. Qiao, “Can we use arbitrary objects to attack lidar perception in autonomous driving?” in *Proceedings of the 2021 ACM SIGSAC Conference on Computer and Communications Security*, 2021, pp. 1945–1960.